Project No. 10-958

Characterization and Modeling of Materials for Kr-Xe Separations

Fuel Cycle

Paul Forster
University of Nevada, Las Vegas

In collaboration with:
Florida Memorial University

Kimberly Gray, Federal POC
Tina Nenoff, Technical POC

NEUP Nuclear Energy University Programs
U.S. Department of Energy

Characterization and Modeling of Materials for Kr-Xe Separations (10-307)

Final Report (Oct 2009 – October 2014)

Name of Project Director/Principal Investigators and associated organizations:
Paul M. Forster, Balakrishnan Naduvalath, Ken Czerwinski (University of Nevada, Las Vegas).

1 Summary

We sought to identify practical adsorbents for the separation of Kr from Xe through pressure swing adsorption. We spent appreciable efforts on two categories of materials: metal-organic frameworks (MOFs) and zeolites. MOFs represent a new and exciting sorbent with numerous new framework topologies and surface chemistries. Zeolites are widely used and available commercial adsorbents. We have employed a combination of gas sorption analysis to analyze gas – surface interactions, computational modelling to both aid in interpreting experimental results and to predict practical adsorbents, and *in-situ* crystallographic studies to confirm specific experimental results.

2 Project Objectives

Several radioactive isotopes, specifically ^{3}H, ^{14}C, ^{129}I, and ^{85}Kr, have the potential to be released in gaseous form during reprocessing of spent nuclear fuel. A comprehensive approach to reprocessing therefore requires that these isotopes be captured and stored until they no longer present a radiation hazard. Unfortunately, there are no practical solutions to several gas-phase separations problems and no generally accepted waste forms for ^{85}Kr. This project specifically addresses the issues associated with radioactive ^{85}Kr and the short lived Xe isotopes that must be captured during the dissolution and processing of fuel. Xe comprises the bulk of the noble gases produced from the fission of ^{235}U, but the isotopes are either stable or decay to stable isotopes over short time scales. ^{85}Kr, on the other hand, has a 10.76 yr half-life. Long-term storage of the mixture is expensive, and release of ^{85}Kr into the atmosphere is unacceptable. An ideal solution would be to separate the Kr for long-term storage (modest Xe impurities would be acceptable), and release or recover the stable Xe. Unfortunately, no technology currently exists that might accomplish this task.

Tasks 1-3 addresses Kr/Xe separations. We surveyed as broad a range of potential nanoporous sorbents for the Pressure Swing Adsorption process as time allowed. A specific emphasis was measuring isosteric heats of adsorption from gas adsorption isotherms collected at a minimum of three temperatures. As promising materials were identified, we sought to understand nature of the gas/sorbent interaction in order to develop a fundamental understanding of the mechanism(s) involved. Understanding specific materials lead to identification of structural features important in producing different adsorption behavior for Kr vs Xe. In Task 4, we examined the feasibility of sequestrating of ^{85}Kr in a nanoporous host. Specifically, we will investigate zeolitic encapsulation with the aim of overcoming the moisture sensitivity of current encapsulates. If successful, this may allow for long-term storage within a concrete-like medium with a pedigree as a waste form.

3 Task Summary

Task 1: Initial Screening – We have developed our experimental approaches to examine sorbents and screened a wide range of sorbents with many different types of pore surfaces. Data from this task has been instrumental in advancing **Tasks 2-3**.

Task 2: Underlying Physics of Gas Uptake – We speculated prior to beginning this project that size selectivitiy and coordinatively unsaturated metal sites were the two most promising pore features to use for this separation. We examined several materials with unsaturated metal sites, and found only modest selectivity in all cases. Detailed examination of HKUST-1 was quite enlightening. While there is an unsaturated metal site, it does not seem to be important in the adsorption at all. Instead, modest initial selectivity is due to a pocket with reasonable size-selectivity. This result highlights the importance of establishing atomistic understandings of adsorption since it would have been easy to infer that the modest selectivity observed was due to the metal center. We have eliminated framework coordinatively unsaturated metal sites from contention in identifying the most promising frameworks.

We have focused on materials with pores/pockets at an appropriate size to provide a close fit for Xe. All of our most promising materials rely on this mechanism for selectivity. Table 1 summarizes the properties of Kr, Xe and CH_4 (which we have considered as a surrogate gas for certain experiments).

	BP/K	Kinetic diameter/Å	Polarizability/$cm^3 \times 10^{25}$
Kr	119.74	3.655	24.844
Xe	165.01	4.047	40.44
CH_4	111.66	3.758	25.93

Table 1: Important physical properties of relevant gasses

We also sought to address the question of whether metal-organic frameworks (MOFs) or zeolites were the better sorbent for this separation. MOFs are an exciting category of materials with widely varying pore sizes and pore composition. Post-synthesis modification, tunability, and high surface areas make them attractive. However, they are generally much less robust than zeolites, would likely be more expensive to use, and are not well established for real-world applications. We put significant efforts also into studying zeolites since, if they were competitive with MOFs in terms of performance, they would be the preferred sorbent for this separation. While zeolite pores are smaller, this is an advantage in some respects for a separation that appears to require size-selectivity.

Mid-way through the project, we recognized the value of molecular modelling for this specific problem. During planning, we had anticipated that modelling the gas surface interactions would be too complicated to be accurately described empirically, limiting us to *ab initio* modelling techniques. Due to the significant time required to carry out and analyze such calculations, we initially saw them as supporting experimental techniques. Midway through the project, we recognized that empirical potentials were able to accurately model gas framework interactions sufficiently well that we could not only use them to help interpret experimental data, but also to predict adsorbent performance. We subsequently worked on developing software to the point it could accurately screen zeolites. While we were not able to complete this work, we are close and anticipate completing and publishing this work in the literature.

Task 3: Targeted Materials Identification/Discovery - Concurrent to the efforts described in **Task 2,** we used the understanding we gained to identify the most promising materials for this separation. **Task 2** results lead us to materials with small pores or pockets as the best means to differentiate between Kr and Xe. For identifying and characterizing MOF materials, we relied on identifying compounds through the literature. For zeolites, we chose to develop and use computational screening methods to identify optimal frameworks and compositions. While this work remains incomplete, our preliminary results suggest that a large number of zeolite adsorbents could be considered for this separation.

Task 4: Kr Encapsulates - Task 4 was partially completed in building a setup capable of carrying out successful encapsulation studies. However, the graduate student working on this project did not pass her advancement to candidacy exams and was forced to wrap up her studies abruptly. She focused on her contributions to the zeolite work in **Task 3** during her short remaining time. This task was peripheral

to the main objectives, and was primarily intended to generate preliminary results that could be followed up on in a later study. We consider replication of literature results a success, but failure to produce advances in this area worth further investigation a disappointment.

4 Summary of Work Performed

4.1 Measuring Heats of Adsorption on the ASAP 2020

A relatively unique aspect of our work is that we focused on measuring isosteric heats of adsorption for Kr and Xe. We anticipated having a commercial setup in place which would allow us to begin quickly. However, a long delay in obtaining the instrument followed by a series of technical problems with the cryostat prevented us from collecting usable data until well into the second year of the project. We were the first US group to utilize a cryostat with this instrument, and ended up hitting a number of issues due primarily to a design flaw in the cryostat which proved both difficult to trace and difficult to convince the cryostat supplier of. We were able to use the time to carry out plenty of literature work and to synthesize many of the sorbents we later studied. Additional details on our extensive efforts to commission this instrument are included in quarterly reports. This was a frustrating problem which slowed our progress since our efforts centered around this technique.

Measuring isosteric heats of adsorption proved to be experimentally challenging. Our general approach was to collect isotherms at three temperatures 10 K apart from each other (20 K range total). This permitted validation of the final heat of adsorption value by 1) allowing calculation of statistics for the fit and 2) allowing us to break the three isotherms into three pairs of temperatures and to then determine HOA values for each of the three pairs. If the HOA values for the three pairs did not match well, we would need to remeasure isotherms. In some instances, problems with agreement between the three isotherms appeared linked to changing degrees of activation of the material.

We also found that it is important to collect isotherms in a relatively narrow range of temperatures specific to the gas we studied. At too high a temperature, insufficient gas loads to be able to determine HOA values for reasonable total loadings. At too low a temperature, much of the adsorption takes place at very low pressures that appear not to be recorded at sufficient accuracy for use in the Clausius Clapeyron equation. The result of the poor pressure readings is artificially low initial heat of adsorption values which gradually track up. This effect disappears when a proper temperature range appears. Our group is collecting material to write a paper detailing how to collect and validate reliable HOA data through gas adsorption.

A more complete record of our gas adsorption work is included in the quarterly reports for this project. For the final report, we highlight the materials which proved either most instructive, or most promising for this separation.

4.2 Synchrotron Microcrystal Diffraction, Powder Diffraction, and Neutron Diffraction with *In Situ* Gas Loading

For success in **Task 2**, precise crystallographic characterization of gas binding sites represents a powerful tool to rationalize gas sorption for a particular compound. We utilized this tool extensively early on in the project, and it served an important role in validating simulations carried out later.

In Dec. 2010, we utilized 12 shifts on the 11.3.1 beamline at the ALS to attempt to locate gas sorption sites in several materials. This is a capability that the 11.3.1 instrument scientist, Simon Teat, is anxious to develop on his beamline. However, the loading cell and procedures for its use are still quite experimental. We selected the metal-organic framework HKUST-1 as well as two novel frameworks recently prepared at UNLV as test compounds. In the first two attempts to dehydrate the crystals on the beamline, it was noted that the compounds failed to dehydrate under the conditions where it was

anticipated they should based on TGA and gas sorption studies. Dehydration was determined by solving the crystal structure and refining the occupancy for solvent molecules. Since heating is accomplished using a warm air stream outside the capillary housing the crystal, we suspected that the heat transfer to the crystal inside of the capillary was sufficiently inefficient under dynamic vacuum that it was not being heated as high as we had anticipated. In the third attempt, we used N_2 gas as a heat transfer medium at elevated temperatures. In this instance, the crystal became amorphous, although the reason for this remains unclear. For a second attempt (May 2011, 12 shifts) we hoped to resolve the previous issues by 1) using N_2 flushes during activation to both improve heating of the sample under vacuum and to remove water through flushing. We also attempted to reduce residual water in the system by adding canisters containing activated zeolite between the gas loading setup and the sample. However, both these improvements proved insufficient to activate the materials with this setup.

Examples of successful refinement of gas sorption sites using single crystal XRD are rare. Most utilize capillary tubes sealed prior to the diffraction experiment. We are optimistic that further development of this cell will lead to the ability to collect data sets with more precisely controlled quantities of gasses, and collect gas loading datasets with multiple gasses (such as Kr and Xe for this proposal) on the same crystal, removing a serious source of potential error. As we had more success with neutron and synchrotron powder methods (below), we did not pursue this technique further. Synchrotron powder X-ray and neutron with *in situ* loading was successful on HKUST-1, and is presented later.

4.3 Gas Sorption Analysis of Kr and Xe in Metal Organic Frameworks

When the cryostat finally became stable in early 2011, we chose HKUST-1 as our first target. In order to test the quality of the heats of adsorption measurements, we decided to study a relatively well-known material with literature heats of adsorption: HKUST-1 also known as copper trimesate. Our intention was to confirm that our instrument is measuring heats of adsorption consistent with the literature, and a recent paper reported heats of adsorption for a number of gasses in HKUST-1. Our intention was primarily to evaluate that our instrument was providing reasonable heats of adsorption. For this reason, we also studied previously characterized gasses including H_2 and N_2. We also chose to do additional noble gasses (Ne and Ar) in addition to Kr and Xe. Noble gas HOAs yet been reported through analysis of gas sorption isotherms, although they have been reported from pulse response measurements.

The HKUST-1 structure proved an ideal material to refine our ability to characterize materials. While the overall structure (Figure 1) is relatively simple, it contains three types of pore surfaces: large hydrophilic cavities of 13 Å (red sphere), slightly smaller hydrophobic cavities (diameter 11 Å), and small hydrophobic pockets approx. 4 Å in size defined b four aromatic rings in a tetrahedral arrangement. We refer to these as" tetrahedral pockets." We note other groups refer to them as "octahedral pockets" since an octahedral arrangement of six Cu_2 paddlewheel units is involved in their structure as well. These pockets are difficult to discern in Fig. 1, but may be more clearly seen from a different perspective in Fig. 2. The two sites most important for understanding gas adsorption in this material are presented in Fig. 2.

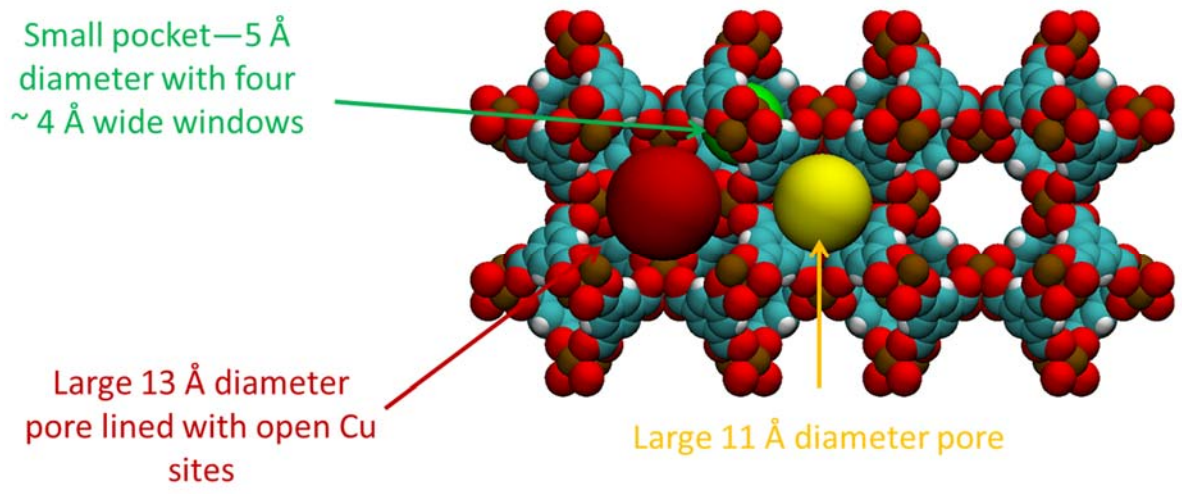

Figure 1. Three different pore surfaces present in HKUST-1

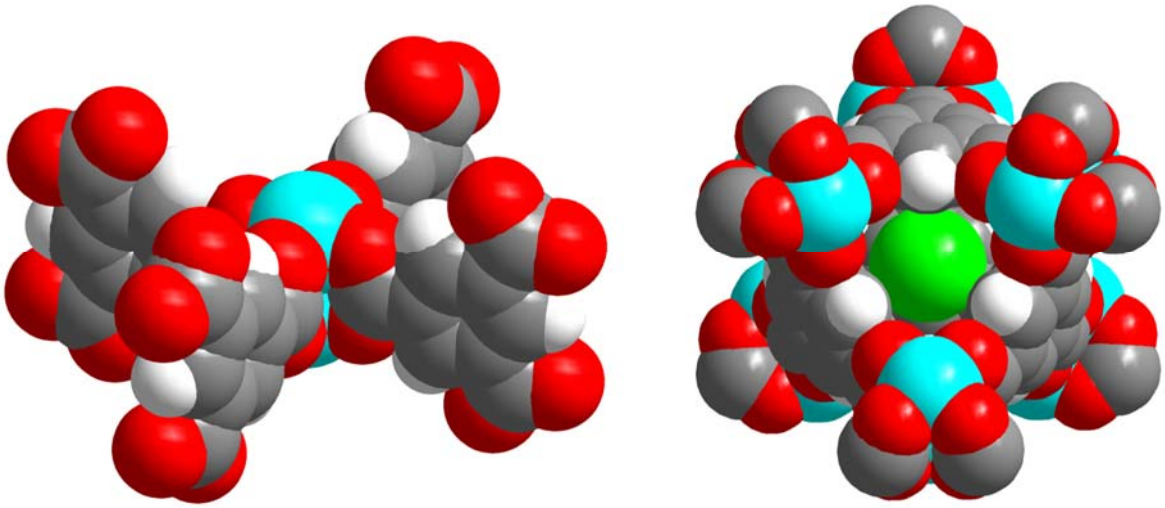

Figure 2. a) A coordinatively unsaturated metal site on a copper(II) atom, as part of the familiar copper carboxylate paddlewheel unit b) Xe (green) in a space-filling view of a cavity with a tetrahedral arrangement of benzene rings.

We anticipated that the coordinatively unsaturated Cu(II) sites, accessible in the hydrophilic cavity, would be the first sites occupied by noble gasses. A number of studies has shown this to be the case for H_2, N_2, and O_2. To summarize our paper on the topic,[i] we found that the primary adsorption site is the center of the tetrahedral pocket. We confirmed this through a combination of studies summarized below.

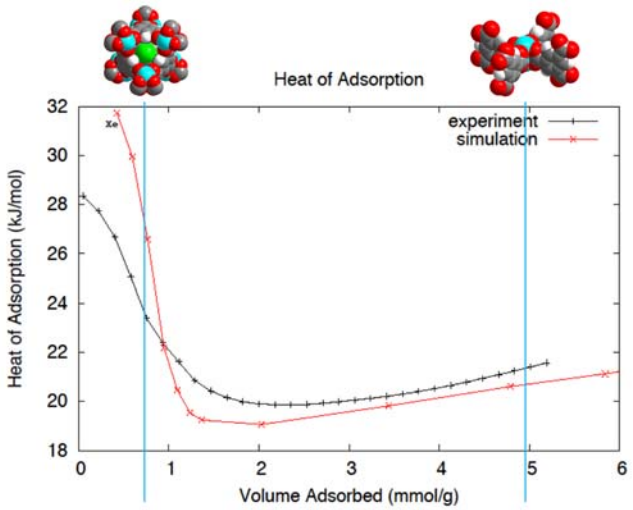

Figure 3. HOA curves measured experimentally (black), computationally (red) show good agreement. High initial HOA values suggest one site is appreciably more favorable than others. Full occupation of the tetrahedral site matches the steepest portion of the dropoff in HOA (1st blue line). Full occupation of the metal sites would match the second blue line.

Figure 3 shows the HOA (simulated and predicted) for Xe in HKUST-1 (Kr results are similar). A key piece of support for the tetrahedral pocket as the primary sorption site is the quantity adsorbed where the HOA drops off. During this study, we became aware of previously published GCMC simulations which provided remarkably close agreement with our experimental data. We contacted the Snurr group, which had performed these publications, and they kindly agreed to replicate them at conditions identical to our experiments (the differences from the previous calculations were minor). As discussed below, this has lead us to develop our own ability to carry out cutting-edge simulations in house.

GCMC simulations are able to show the positions occupied by gas atoms during the adsorption process. If there is also close agreement between experimental and simulated isotherms and HOA values, there is good reason to be confident that the simulation represents a reasonable approximation of what is actually occurring during the experiment. This information is invaluable in establishing structure-property relationships for adsorbents and for explaining why certain adsorbents offer better selectivities than others. Examples of predicted gas densities are shown in Figure 4 below.

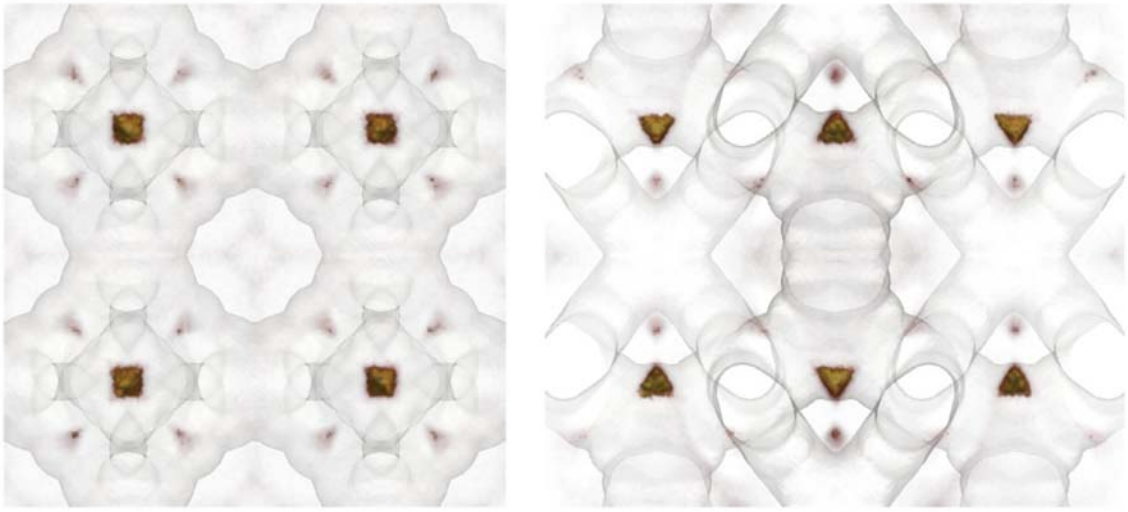

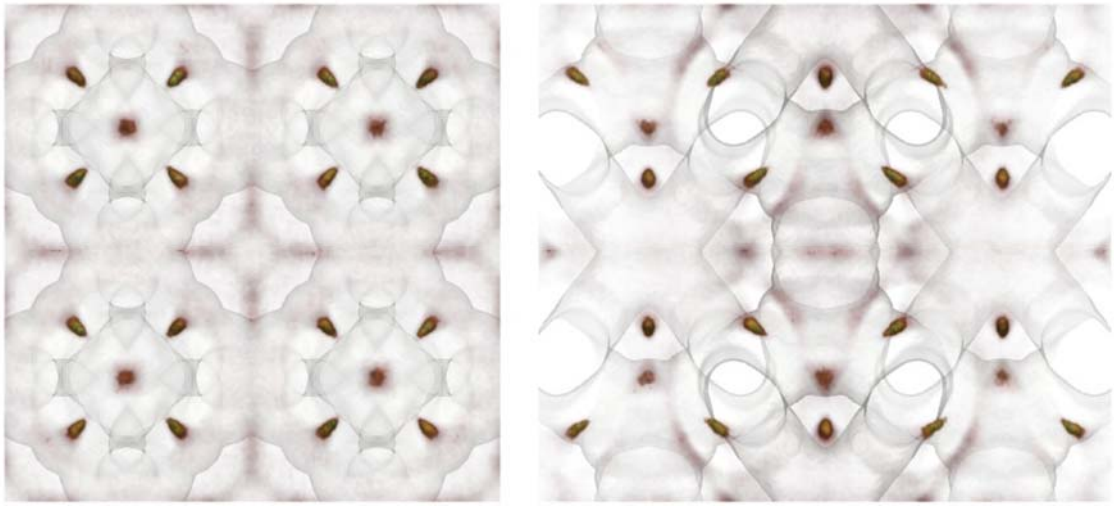

Figure 4: Maps for simulated Xe density in HKUST-1 at low and high loadings. The two top figures represent modest loadings viewed from two different directions; the bottom two figures represent a loading corresponding to about 20 atm.

We carried out calorimetric work collaboratively with Alex Navrotsky (U.C. Davis). Her calorimetric results were quite close to our HOA value determined through the Clausius Clapeyron, confirming the validity of our experimental approach. We also carried out detailed crystallographic studies in cooperation with Craig Brown (NIST). The major important outcome is that the crystallography showed identical trends to the adsorption behavior that we had already deduced through the GCMC simulations.

Synchrotron X-ray powder diffraction (XRPD) data for Xe and Kr loaded samples were collected on beamline 17-BM at the Advanced Photon Source at Argonne National Laboratory, and neutron powder diffraction (NPD) data for Ar loaded samples were collected on the high-resolution BT-1 diffractometer at the National Institute of Standards and Technology Center for Neutron Research (NCNR). Rietveld refinements were performed on data for both the bare framework and the material dosed with various amounts of each gas after locating the adsorbed atoms using Fourier techniques. Values of refined site occupancy factors (SOF) for the various adsorption sites are converted to volumetric quantities for easier comparison of the structural data to the heat of adsorption curves. For all three gases, there is no evidence of any binding at the open Cu sites; all binding sites are within and around the small pockets.

The structure determined for the lowest loading of Xe (0.357 mmol/g) confirms that the primary adsorption occurs at the center of the pocket, located approximately 4.5 Å from the center of the tetrahedrally arranged benzene rings, which define the pocket wall (Figure 8). A secondary binding site is

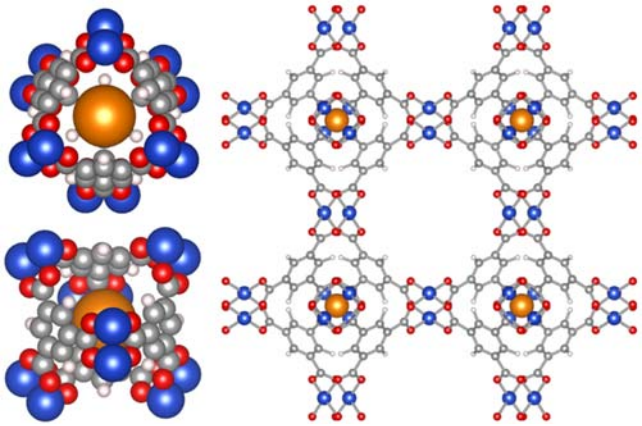

Figure 5. View of HKUST-1 showing the strongest binding site for Xe (orange atoms) at the pocket center, with two views of the small pocket isolated (top left and bottom left) and view of one unit cell down the *c*-axis (right).

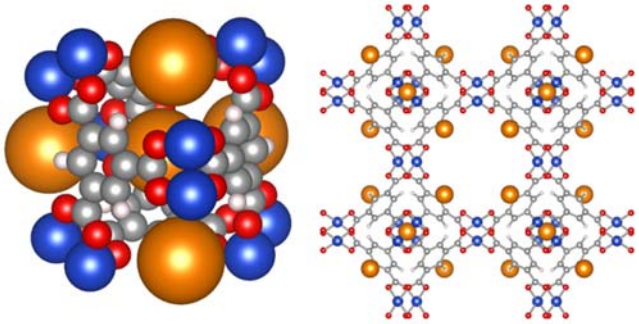

Figure 6. View of HKUST-1 showing secondary Xe binding site (orange atoms) at the four windows to the small pockets as well as the pocket site (one pocket isolated on the left, and view of one unit cell down the *c*-axis on the right).

determined to be at the windows to these pockets (the "window site") that starts to be occupied before the pocket site has completely filled (Figure 6).

The window site is at the center of the triangular window tetrahedrally located around each pocket with each site being symmetry equivalent. The shortest Xe-framework contact for the window site is with the three ligand H atoms. While the atomic displacement parameters (ADP) are relatively large, reflecting the thermal motion and potential site disorder, there is a gradual change in the fractional coordinate of the window Xe atom, moving towards the center of the pocket and resulting in a shorter Xe-Xe distance with increased loading (Xe-Xe distance ranges from 6.04(3) Å to 5.19(1) Å). Once adsorption at the window site is observed, both the pocket and window sites populate at similar rates for successive dosings (Table 2).

Partial occupation of the secondary, lower energy window site prior to full occupation of the pocket site displays excellent correlation with the experimental heat of adsorption data (Figure 7, left). Heat of adsorption values are very high in the region of dose 1, where adsorption is observed exclusively in the pocket. The sharp decrease in measured heat of adsorption begins as the window sites begin to occupy, and eventually levels off around dose 5, when the pocket site is almost fully occupied. This structural data is also consistent with the adsorption

Table 2. Refined SOFs for Xe sites as a function of loading amounts. Values in parentheses indicate one standard deviation in the refined value.

Dose	Xe adsorbed per Cu	Xe adsorbed per pocket	Xe adsorbed (mmol/g)	Pocket site SOF	Window site SOF
1	0.072(1)	0.432(4)	0.357(3)	0.432(4)	0
2	0.160(2)	0.96(1)	0.79(1)	0.670(4)	0.072(3)
3	0.187(2)	1.12(1)	0.93(1)	0.757(4)	0.091(3)
4	0.207(2)	1.24(1)	1.03(1)	0.799(5)	0.111(3)
5	0.315(2)	1.89(1)	1.56(1)	0.930(6)	0.240(3)

Table 3. Refined SOFs for Kr sites as a function of loading amounts. Values in parentheses indicate one standard deviation in the refined value.

Dose	Kr adsorbed per Cu	Kr adsorbed per pocket	Kr adsorbed (mmol/g)	Pocket site SOF	Window site SOF
1	0.075(1)	0.449(8)	0.371(6)	0.112(2)	0
2	0.184(3)	1.10(2)	0.91(1)	0.175(2)	0.100(4)
3	0.372(4)	2.23(2)	1.84(2)	0.242(3)	0.316(5)

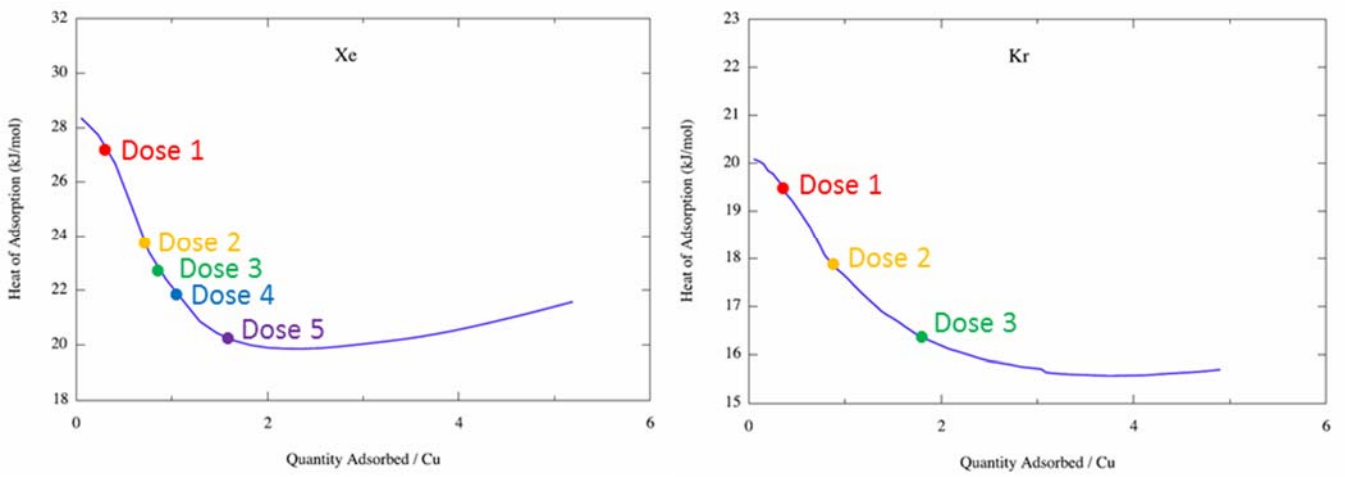

Figure 7. Experimental heat of adsorption data with overlaid dose amounts for Xe (left) and Kr (right).

positions predicted by the GCMC simulations (Figure 5(c) corresponds to loading levels near dose 5). Additional powder patterns were collected for expected loadings of 0.5 Xe per Cu and higher where lower energy sites are expected to be apparent, however a significant increase in background and decrease in peak intensity makes XRPD structure refinement ambiguous, as electron density contrast between the framework and Xe in the pores is reduced. This implies that at these moderate loading levels adsorbed Xe atoms do not preferentially occupy well identifiable sites and that Xe is effectively condensing on the pore surfaces. This observation is consistent with both the leveling off of experimental heats of adsorption in this range and the molecular simulations which do not predict well-defined binding sites within the large pores at moderate and high loadings of Xe.

Site preferences for Kr determined from XRPD data are similar to that of Xe, with slight differences in the refined locations of the pocket and window sites that we use to describe the adsorbed locations of the noble gas atoms. The initial, strongest binding site is also within the small pocket, however as Kr is slightly smaller than Xe, it does not occupy the center of the pocket. More efficient potential interaction with the pore surface is possible at a slightly off-center position within the pocket (Figure 8, left), with a closest Kr-C distance of 3.95(2) Å. This illustrates one reason why the heat of adsorption at the lowest loadings is considerably lower for Kr than Xe; the Xe atom at the center of the pocket interacts with the benzene rings from all four ligands, while the Kr atom is only interacting with three. The Kr pocket site is disordered over four locations within the pocket, and only one Kr atom can fit inside at a time.

Occupation of the secondary window site occurs in the same volumetric uptake region with similar relative fractional occupancies of the sites for Kr as is observed for Xe (Table 3). The window site is similarly at the center of the window (Figure 8,

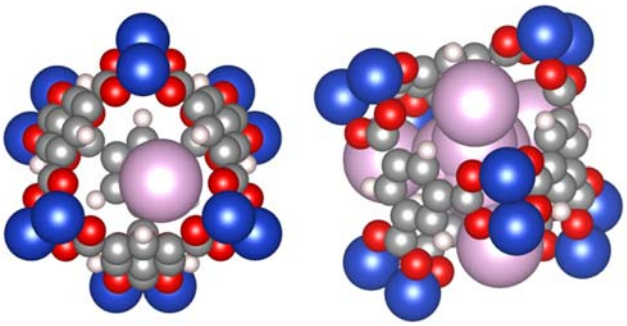

Figure 8. Binding sites for Kr (pink atoms) in and around one pocket of HKUST-1. View on left shows pocket site that is slightly shifted from the center of the pocket (only one of the four symmetry related pocket sites is shown); view on right shows the secondary window site with all four possible locations of the pocket site.

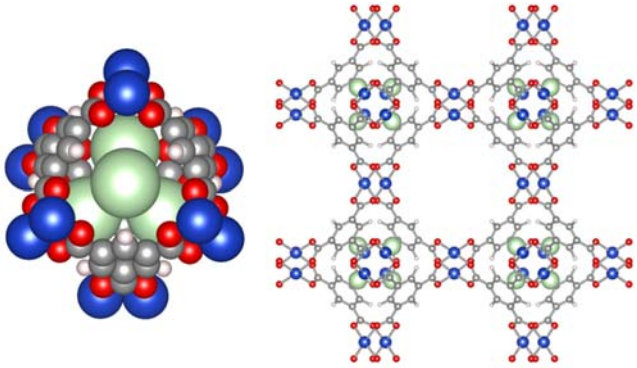

Figure 9. Binding sites for Ar (green atoms) inside pocket windows in HKUST-1. View on left shows one isolated pocket looking through the window at the four Ar atoms arranged within the pocket; view on right shows one unit cell viewed down the *c*-axis to reveal the primary binding site.

right) with the shortest framework contact at the ligand H atoms. In dose 2, the Kr-Kr distance is 4.40(3) Å. In dose 3, the window site moves closer to the center of the pocket, to the extent that occupation of the window site does not allow simultaneous occupation of all four symmetry related pocket sites. At this loading, the Kr pocket site can either be modeled at the center of the pocket with a very large ADP value, or split into the four disordered sites slightly off-center with a more reasonable ADP value. We have refined the structure using the latter model, where the Kr-Kr distance of 4.63(2) Å represents the distance from the window site to the three pocket sites closest to opposite windows. Adsorption at the lower energy window site with increased loadings correlates well with the decline in observed heat of adsorption (Figure 10, right). As with Xe adsorption, XRPD data collected at higher expected loadings for Kr display an increase in background and decrease in peak intensity that makes structure refinement ambiguous, indicating that at moderate loading levels adsorbed Kr atoms do not occupy well-defined sites.

Assignments of Ar adsorption sites inferred from the experimental adsorption data and molecular simulations were confirmed by neutron diffraction experiments. At a loading of 0.18 Ar

per Cu, adsorbed Ar occupies a site essentially between the window site and the central pocket site as described above (Figure 12). This allows for close contacts with the ligands forming the pocket surface, with Ar-Ar distances (4.02(7) Å) large enough such that four Ar atoms can fit within the pocket at once. The refined Ar positions are in nearly identical locations as the predicted locations from the molecular simulations.

While we do not believe that HKUST-1 is a particularly good adsorbent for Kr/Xe separations, our detailed study has produced a large number of important results, especially for further efforts by our group. Firstly, these results provide a very compelling example of the utility of GCMC modelling for this particular problem. The modelling is imperfect, but provides an excellent tool both to predict and explain sorption in a wide range of systems. This system convinced us to switch from an approach that was experiment lead, where simulations were used to interpret data, to one where simulation lead us to materials worth studying experimentally.

This system also provided an excellent means to refine our ability to carry out GCMC reliably. One issue that we found is the critical role played by the crystal structure used in the simulation. Since we had access to a number of experimental structures for HKUST-1, we were able to test our simulations against the structures. We chose to use the original structure and 11 structures with various amounts of noble gas present. This structure is probably the least reliable because it was collected on a fully solvated crystal and solvent and coordinated water molecules were simply deleted. Differences between the 11 desolvated structures collected either under vacuum or with various species sorbed were relatively minor. To our surprise, we found that GCMC simulations predicted appreciably different sorption behavior between all of the samples (Fig. 10). This was **not** due to random variations in the structure, but due to slight framework changes in the structure that occurred in response to gas adsorption, as we were able to establish in a short paper on this topic.[2] This result is quite significant because it demonstrates that framework flexibility remains important even in apparently rigid materials like HKUST-1. It lead us to develop better methods to include framework flexibility into our in-house GCMC package. We also concluded that the flexibility tended to improve selectivity for the more strongly sorbed species, suggesting some degree of flexibility could be beneficial overall in a sorbent.

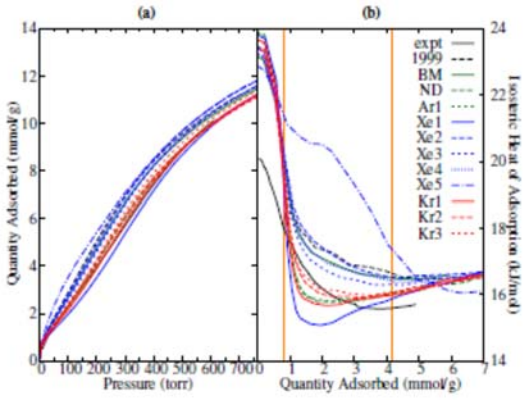

Figure 10: Simulated adsorption isotherms and HOA values for 12 different experimental crystal structures. Appreciable differences in simulated HOA are evident.

Learning which site is most efficient for Kr/Xe separations in HKUST-1 lead us to consider size selectivity as the most promising feature with which to separate these gasses. For the remainder of the project, we targeted this as our primary means to distinguish the two gasses.

Our next major study concerned transition metal formates. This family of materials is the alpha phase of the M(II)-formates. The work focused primarily on the two metal centers: Ni and Co. We were able to successfully synthesize and obtain good surface areas for these materials. The work followed our combined experimental/simulation approach comparing heats of adsorption based off of single gas adsorption isotherms. The structure for the Ni form is shown in Fig. 11 below:

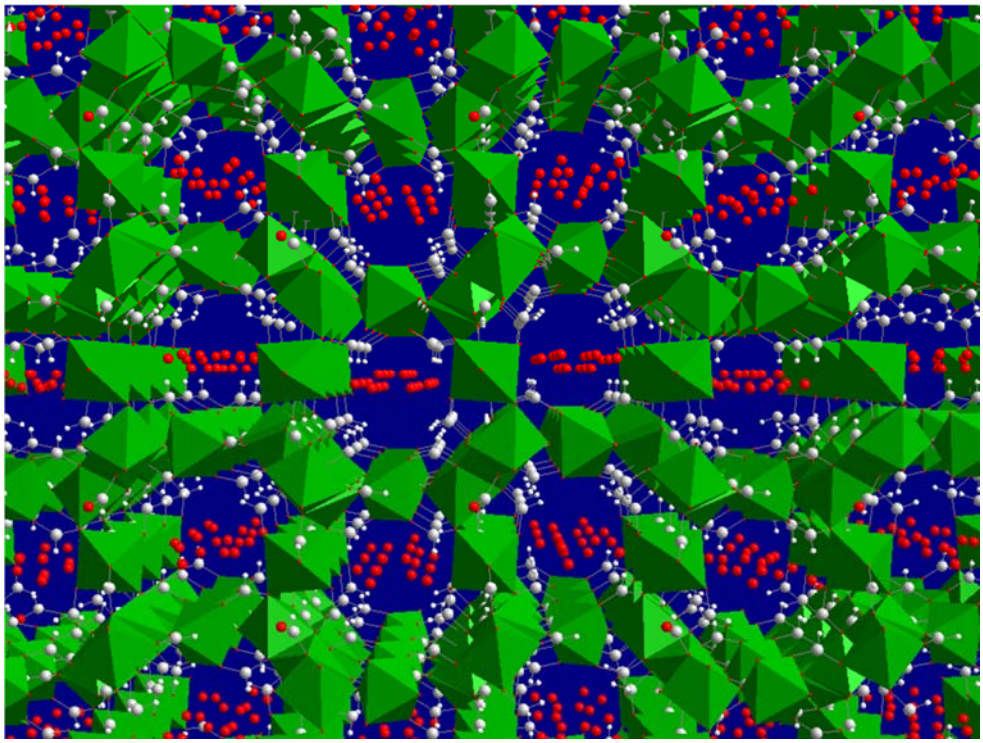

Fig. 11 The structure of nickel formate with NiO_6 octahedra in green and solvent water molecules in red.

Simulation provided excellent agreement with our gas sorption experiments (Fig. 12). Good agreement strongly suggests that the simulations are accurately matching the actual gas adsorption process and may be used predictively in this system.

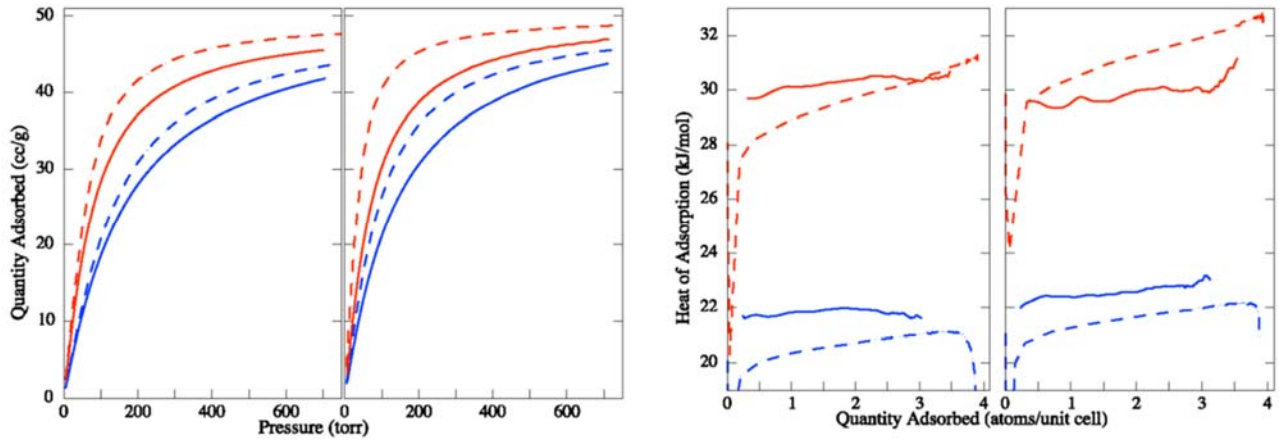

Fig. 12 Simulated (dashed) and experimental (solid) gas sorption isotherms (left) and heats of adsorption (right) for Kr (blue) and Xe (Red) in nickel and cobalt formates.

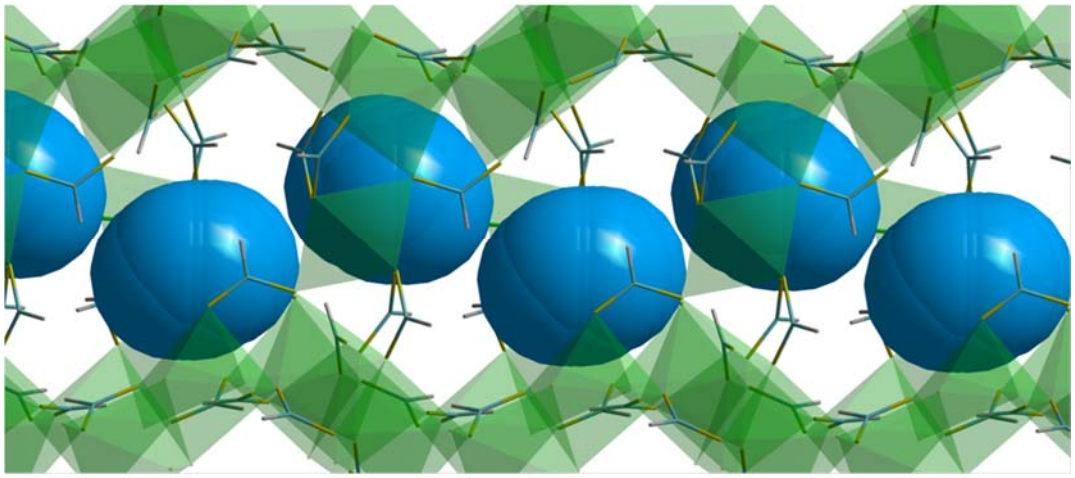

Fig. 13 Simulated most probable positions for noble gas atoms. The gas is reasonably localized in a single crystallographically identical site, leading to flat HOA values as a function of loading.

Since the HOA values are pretty consistent across all loadings, the selectivity is also quite constant. This is a major reason why we do not consider HKUST-1 to be a particularly promising sorbent. It may have a slightly higher initial selectivity, but the selectivity drops dramatically as the single, selective site becomes occupied. Because the secondary adsorption sites have only modest selectivity, the material overall performs poorly. This stresses the importance of characterizing a material past the initial selectivity, which is all that many methods (such as breakthrough curves) are able to provide. Selectivities for cobalt formate are compared with HKUST-1 in Fig. 14

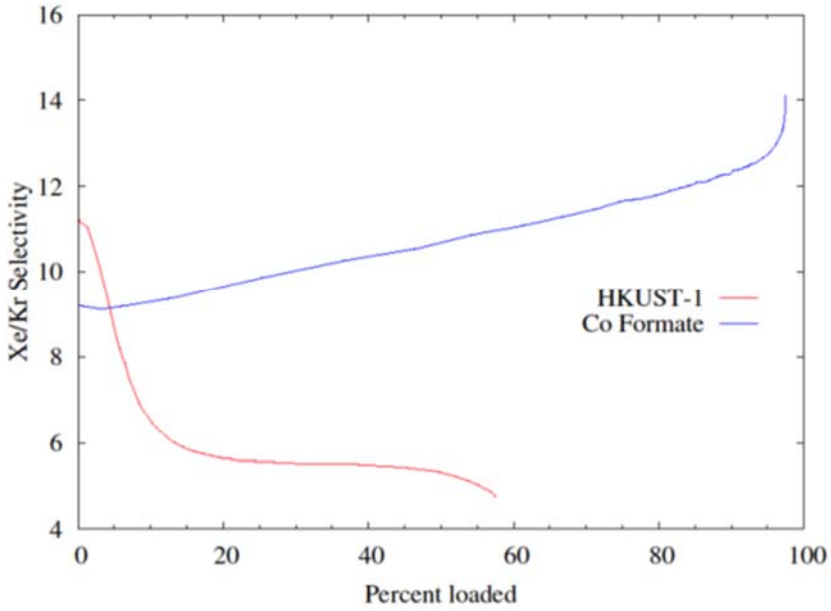

Figure 14. Selectivities for cobalt formate compared to HKUST-1 as a function of loading (experimental values determined with IAST)

The LJ gas–gas interactions between adjacent Xe sites separated by 5.35 Å interaction is 1.2 kJ mol_1. Not surprisingly, the magnitude of the increase for the calculated curves is essentially identical to what we predict with this reasoning (2.4 kJ/mol). While the increase seen experimentally appears somewhat less pronounced, it is noteworthy that all four HOA curves slope upward. Simulations with no gas–gas interactions produce nearly flat HOA curves. For practical separations, a large difference in HOA between two gases suggests a sorbent will show high selectivity, as previously demonstrated for HKUST-1.

The unusually flat HOA curves suggest very even selectivity over a wide range of loadings. Isotherms for Kr and Xe in 1 at 250 K were measured to estimate selectivity. In the low loading range, Henry's law constants were around 20 times greater for Xe than Kr, consistent with the high selectivity. While these materials have lower surface areas and gravimetric adsorption capacities compared to some other MOFs, their porosity is on par with zeolites which are already used extensively in gas separations. In conclusion, nanoporous metal formates exhibit excellent. Challenges to adapting these materials as adsorbents will include scale-up of the synthesis and forming these materials into pellets compatible with real-world gas adsorption systems. The synthesis are robust and work well for lab-scale quantities (grams), but have not been scaled up to our knowledge. This work is described in detail in a publication.[3]

4.4 Progress on Simulations and Experiments for Separations Using Zeolites

Zeolites present a very different set of challenges compared with metal-organic frameworks in terms identifying the best sorbents. However, given their commercial familiarity, low costs, generally excellent stability, and low toxicity, they would be the preferred sorbent over metal organic frameworks should they prove to have competitive performance.

We began with an experimental investigation of zeolites we considered representative of the family overall with the aim of finding features in certain materials that would guide us to better sorbents among the many framework types, Si/Al ratios, and extra-framework cations possible.

A short summary of our experimental findings on zeolites is presented. Further details are present in Breetha Alagappans thesis "Assessing Different Zeolitic Adsorbents for their Potential Use in Kr and Xe Separation."[4] In short, the initial experimental studies showed that adsorption is complicated in zeolites. As we recognized the utility of GCMC simulation, we decided to reapproach the problem from a computational perspective. While we were unable to complete this during the award period, we have made considerable progress, and will continue working on our approach.

Within a fixed zeolite structure and Si/Al ration, the heat of adsorption appears to vary primarily based on the gas-cation interaction. For lighter gasses, polarizability appears to be the most important interaction and so smaller cations lead to higher heats of adsorption. Thus, for Li-Na-Kr, Ar has the highest HOA for Li-containing zeolites. For heavier noble gasses like Xe, the opposite trend is observed, suggesting that dispersion interactions are a more important contribution to the total HOA. For Kr, the HOA does not vary much at all for all three cations, suggesting both contributions are about equally important.

By plotting the observed initial HOA as a function of the non-constant terms in calculating the polarization and dispersive interactions, these trends become apparent in the figures below. The result is significant. Exchanging heavier monovalent cations into zeolites improve their HOA for Xe while lowering it for Ar. Kr appears more weakly affected, although it is a challenge to interpret results for partially exchanged Rb and Cs samples (full exchange for LSX appears impossible for these cations based on a literature survey). We are planning to look at zeolites with higher Si/Al ratios where full exchange is possible soon to confirm this finding and properly extend it to Rb and Cs. Results are summarized in Figures 15-16.

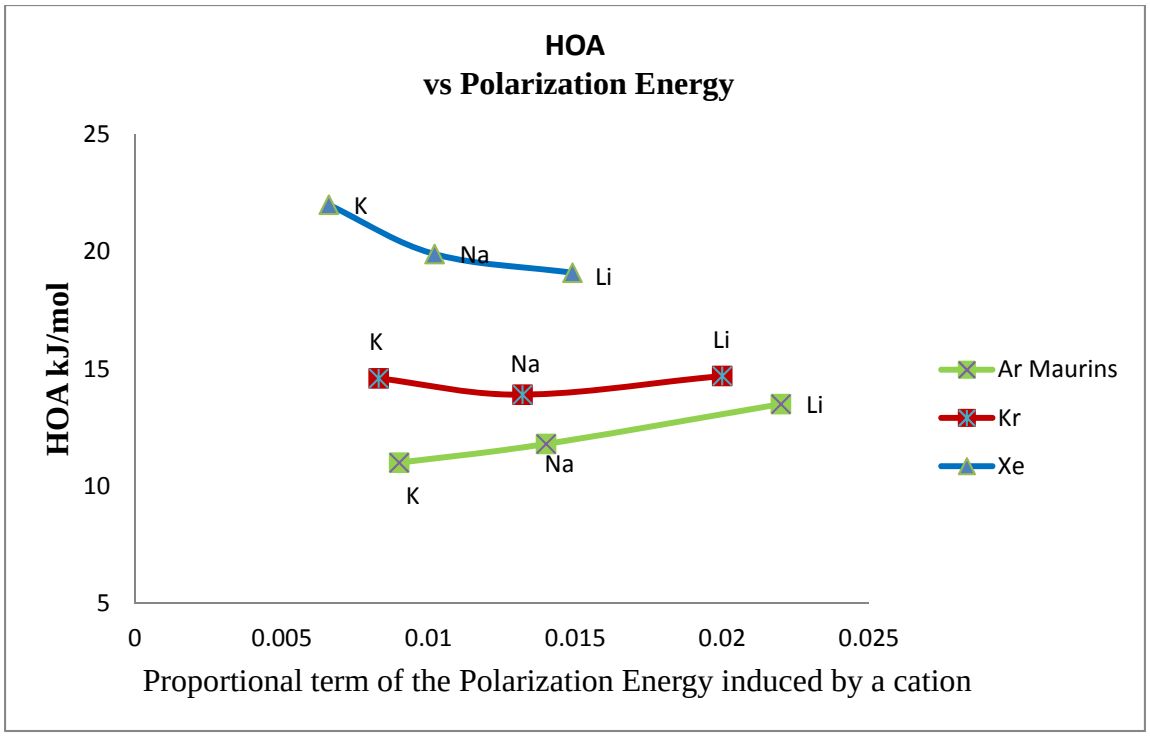

Figure 15. Proportional term of the polarization energy vs. HOA in Ar (Maurin's), Kr and Xe with Li, Na and K cations.

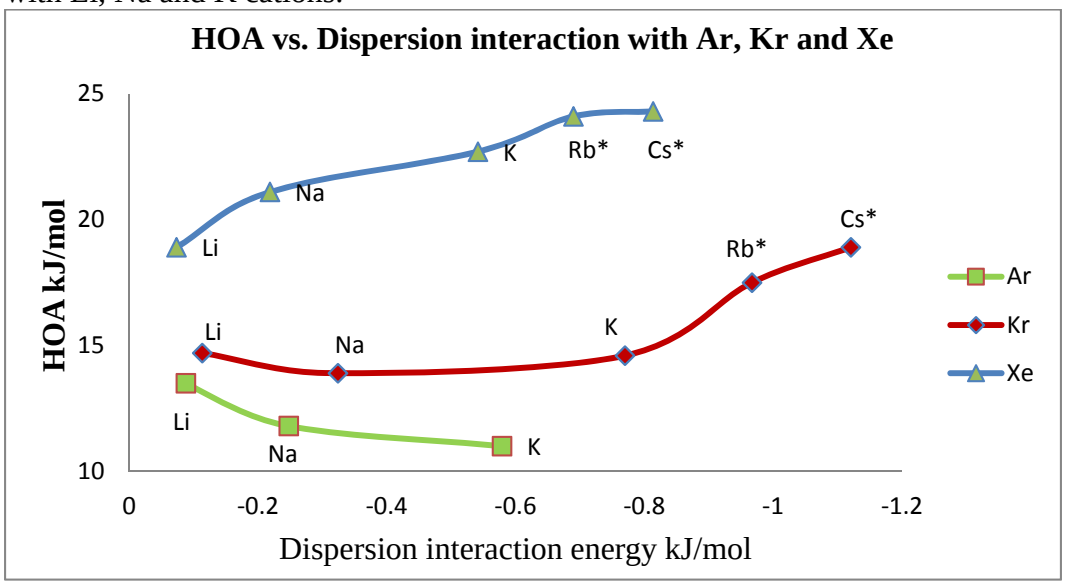

Figure 16. Ar, Kr and Xe dispersion interaction with the alkali cations in the zeolite frame work vs HOA

Due to the large possible numbers of zeolites, the added complexity (compared to MOFs) of extra-framework cations, and the challenge of synthesizing large numbers of them, we adjusted our approach to simulation rather than experiment. A description of an as-yet-unexplained experimental finding should highlight the complexity of the simulation challenge. Gas sorption analysis into Li, Na, and K ion exchanged faujasite (FAU) yielded unusual HOA curves that abruptly jump up by several kJ/mol. An abrupt rise made no physical sense unless some phase change had occurred, but none are known for the FAU structure. The structure is sufficiently well documented that a structural phase change is unlikely. We initially attributed this to experimental issues, but they persisted in multiple runs that could not be explained by experimental error.

Re-evaluating these curves at higher resolution in both the adsorption and desorption and confirmed unusual behavior. The isotherms begin with an initial slope indicative of a heat of adsorption and then abruptly kinks up by several kJ/mol over a relatively small loading range. Generally, increases in HOA as a function of loading are known, but usually attributed to gas – gas interactions. That cannot explain these observations because the rise is too steep, and occurs at too low a loading to be realistic. Hysteresis present around these loadings does not improve with higher analysis temperatures, as we typically observe. For both FAU-K and Na we observed these loops for the adsorption gases Ar, Kr, and Xe. The pores in FAU are large and framework flexibility is unlikely. Additionally, the total desorption curve for the 'high capacity' material is within 1 cc/g of the adsorption indicating a normal within parameters leak rate of the system. The best explanation is of an internal structural change once the adsorbed gas reaches a certain critical density which gives the gas adsorbate better access to the more energetically favorable internal surface of the zeolite. Many materials frameworks actually deform and change lattice coordinates under these stresses, but this has yet to be reported for FAU. The simpler answer is the adsorbed gas once at its critical density has strong enough forces acting upon it to move the cation out of the way particularly from the favorable cation sites right in the middle of the windows between the different alpha and beta cages. As described in the previous quarter we made several revisions and efforts in order to model the gas sorption into zeolites.

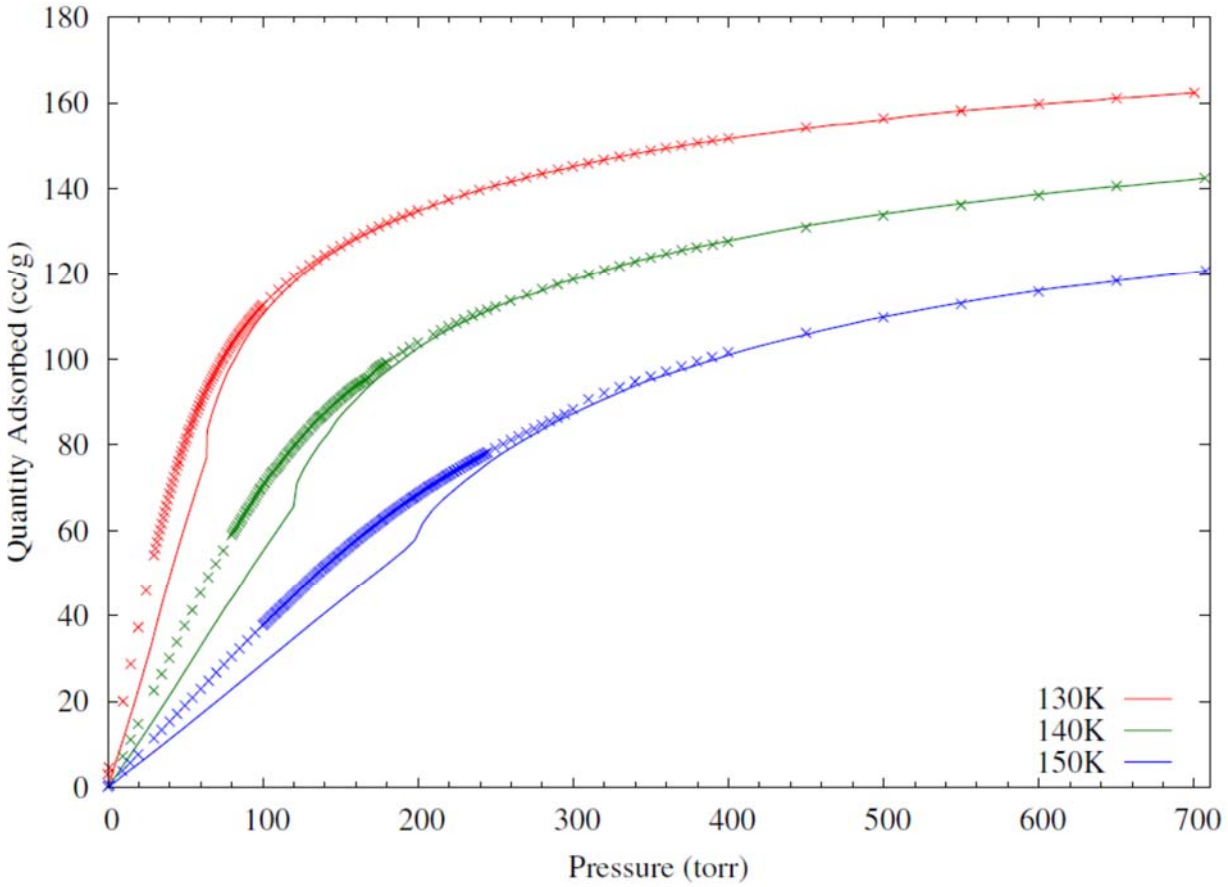

Fig. 17 As-yet unexplained isotherm behavior for Ar. Similar behavior is evident for other gasses, including Kr and Xe, but we are best able to show it for the FAU sample.

If cation mobility is a part of this, it raises the complexity of simulations greatly. The basic problem is that cations moving to appreciably different positions usually depend on coupled movements of cations and also require gas atoms to move. Producing the necessary set of GCMC moves through standard GCMC moves is sufficiently improbable that equilibrium is nearly impossible to achieve. Based on consultation with John Low (ANL), we set out to add coupled jump moves which have previously been effective for simulations with other problems requiring cation mobility. These moves are nearly implemented, but not yet complete.

While working on cation mobility, we recognized we needed to be certain we had the framework gas interaction correct before we would verify we were correctly simulating the gas-cation interactions. We chose to study purely SiO_2 zeolites to confirm our approach. This work has recently been published;[5] we present a brief summary here.

We carried out extensive Kr/Xe simulations of Kr and Xe isotherms, heat of adsorption, and selectivity for purely siliceous versions of all 229 currently recognized zeolite frameworks. A major part of this effort was extensively evaluating a number of potentials for all relevant atom-

atom interactions and selecting ones that both made the most physical sense and best matched three SiO_2 zeolites we evaluated experimentally. Extensive explanations of the screening methodology, programming for our cavity mapping software, and other details are included in the manuscript.

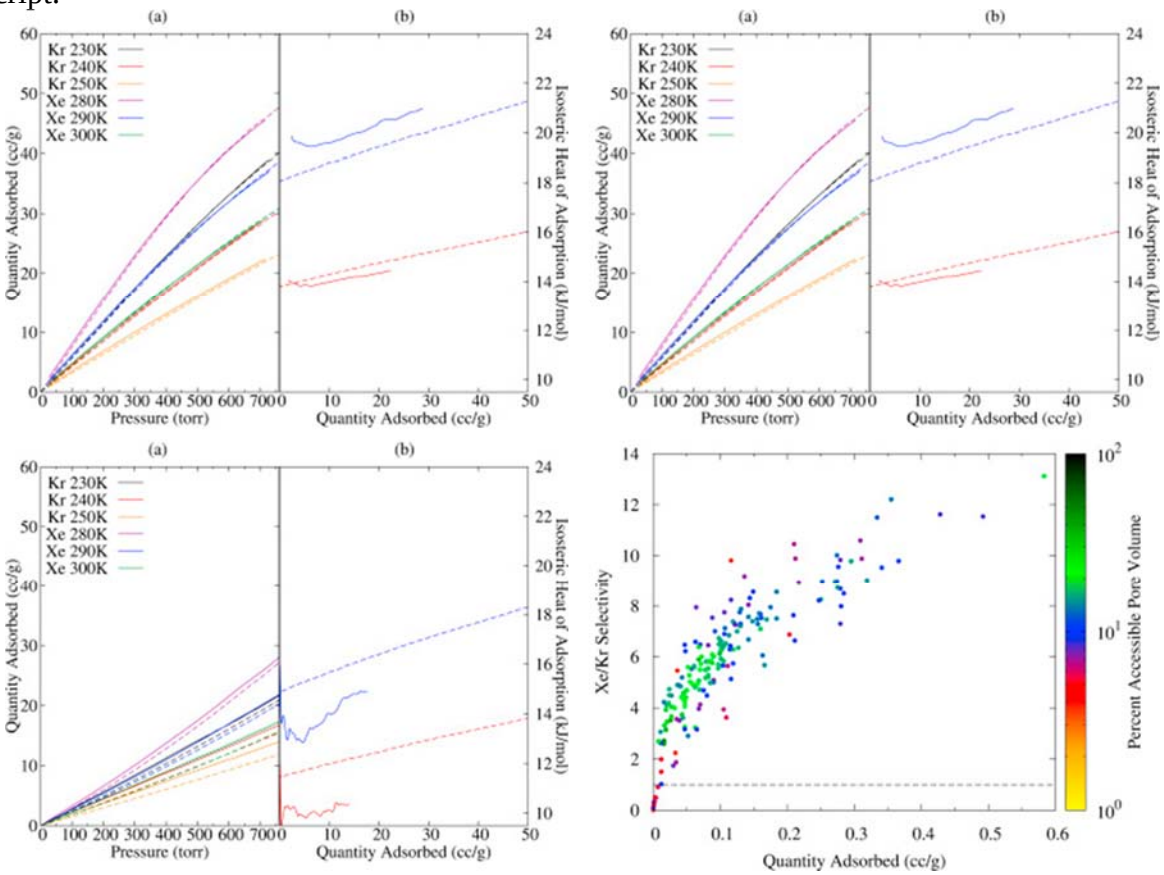

Fig. 18: Boxes a), b), and c), compare simulated isotherms (left) and HOAs (right) for zeolites LTA (a), BEA (b), and FAU (c). Experimental and simulated curves are solid and dashed, respectively. D) presents a plot relating the loading with selectivity for low pressures (1 torr)

Figures 18 contains our experimental and simulated isotherms and heats of adsorption for LTA, BEA, and FAU plotted on the same scales for easy visual comparison. These are the SiO_2 zeolites selected for comparison of computational and experimental data. The simulated heats of adsorption were found using fluctuation theory at the same median temperature used in the determination of the experimental heats of adsorption. BEA (Figure 18b) is known to be polymorphic, and we only performed simulations using the structure of polymorph A, the most representative polymorph. Given the similarity between the BEA polymorphs, we did not anticipate large differences with this approximation, as confirmed by the close agreement encountered. FAU is known to be a difficult material to produce in its purely siliceous form, as the process require dealumination and can lead to mesoporosity and aggregates of amorphous silica. This FAU sample seems to be high quality as a 77K N pore size distribution (over the default range

in the Micromeritics software) is trimodal, which is in line with the three primary topological features of FAU: the *alpha* cage (t-fau), sod(t-toc) the sodalite or *beta* cage, and d6r (t-hpr) connecting the sodalite cages. The agreement between the FAU HOAs is of comparable quality to that of LTA and BEA, however the simulation model under-predicts total adsorption by 5-10%. We believe the discrepancy arises from two factors: the mass of the measured sample being too low giving too high measured quantities adsorbed, and the COMPASS fluid-fluid parameters being too weak as FAU is a large pore system where correctly describing fluid-fluid interactions will be more critical.

The finalized model we employed yields excellent agreement for the isotherm and heat of adsorption for both gases at all tested temperatures. The predicted and measured heats of adsorption are both fairly flat, as expected of the relatively homogenous surface inside these zeolites. What is surprising is the similarity of the predicted heats of adsorption for Kr and Xe in both materials. A lack of small accessible pockets in the cells and a surface covered in 4-ring to 6-ring provides an easy explanation for the flatness and similarities in the heats of adsorption between these materials. The difference in heat of adsorption is consistent across all loadings which we have shown indicates a fairly uniform Xe/Kr selectivity at all loadings will be observed. We recognize that our approach neglects structural changes in response to gas uptake, as are known to occur in MFI, for example. However, the initial selectivities obtained from our calculations should still be valid.

We carried out our screening at 298 K at five pressures on a logarithmic scale spanning the Henry's law region (1 mmHg) to PSA useful pressures (10,000 mmHg). Figures 18d summarizes the screening results for the initial adsorption (1 mmHg). The selectivities presented are for Xe over Kr, and the material's percent accessible pore volume is used to shade the plotted points. A strong correlation between total loading and selectivity is evident. The total quantity adsorbed is primarily determined by the affinity of the zeolite for noble gases - frameworks with high HOAs for Kr and Xe also tend to have high selectivities. It is promising that zeolites with the highest selectivities tend to have relatively high adsorption for Kr and Xe as well. It is noteworthy that 10 zeolites have selectivities in excess of 10 - a value comparable to the most promising MOFs studied so far.

For some separations, a selectivity in favor of Kr is desirable. A recent review of MOF applicability to this problem highlighted FMOFCu, which could go from being Xe selective to Kr selective by lowering the temperature below 0 °C.[6] A few siliceous zeolites appear selective for Kr (Xe/Kr selectivity less than 1), but none appear practical overall. At 298 K , four Kr-selective materials exhibited reasonable total gas loadings (40 cm^3/g), yet they are only slightly selective for Kr. More selective frameworks all have low porosity and either modest uptake or low Kr selectivity at the highest pressures measured. Additional simulations at a lower, yet potentially realistic PSA temperature (250 K), were performed to see if the loadings of the Kr selective materials could be improved. Table 4 shows the results for quantity adsorbed and Kr selectivity at the highest loading point (10,000 mmHg) for both temperatures evaluated. When cooled, the quantity adsorbed improved by no more than a factor of 5 for each of the zeolites examined. The Kr selectivity did not change appreciably for any materials with reasonable loadings. Remarkably high Kr selectivity is suggested in several topoligies, including CHI and NPO, but the predicted total uptake is so small that these materials would be impractical for applications. Our simulations strongly suggest no siliceous zeolites would be competitive with FMOFCu.

Simulated Total Quantities Adsorbed (cm3/g) and Kr/Xe selectivities for initially Kr selective zeolite framework types calculated at 10<comma>000 mmHg at both 298 K and 250 K.					
Code	298 K	250 K			
N (cm3/g)	SKr/Xe	N (cm3/g)	S electivityKr/Xe	N (cm3/g)	
ABW	1.42	48.44	5.84	39.85	
ACO	76.58	1.68	134.68	1.3	
AEN	2.46	9.12	10.09	8.97	
APC	4.15	9.48	18.36	10.66	
BIK	2.01	13.85	7.66	15.59	
CHI	0.11	214.98	0.29	470.88	
CZP	14.27	3.59	36.22	3.88	
JBW	7.89	5.13	26.62	5.43	
LTJ	2.3	11.41	10.34	12.94	
MON	2.44	14.27	10.38	14.61	
NAB	0.98	16.42	2.35	107.5	
NAT	69.63	0.91	101.08	0.74	
NPO	0.3	76.32	0.84	148.52	
NSI	0.56	43.63	1.87	75.53	
PAR	0.99	14.46	3.34	14.69	
RRO	12.26	2.78	33.97	2.85	
RWR	35.48	1.91	83.39	1.53	
VSV	6.5	3.68	19.94	4.04	
WEI	1.93	20.88	7.59	18.39	
YUG	30.52	1.11	43.57	1.03	

Table 4: Summary of data related to observed Kr selectivity. Materials either have very low uptake, or too low a selectivity to be meaningful.

Figure 19 shows a strong correlation between the initial selectivities compared against the difference in the Xe and Kr heats of adsorption into the material. The heats of adsorption were computed with multi-component fluctuation theory. There appears to be a maximal initial selectivity possible for a given difference in initial HOA, although many materials show lower selectivities than this. Normalizing the difference in heat of adsorption to either the Kr, Xe, or total heat of adsorption does not yield a more linear or tightly correlated data set. The same effect is observed at all loadings with a similarly narrow spread in the results. This plot directly demonstrates the established rule of thumb for using single gas adsorption measurements to

estimate a material's selectivity. Figure 19 indicates that, for a material to have a Xe selectivity > 10, the difference in heat of adsorption needs to be > 8 kJ/mol.

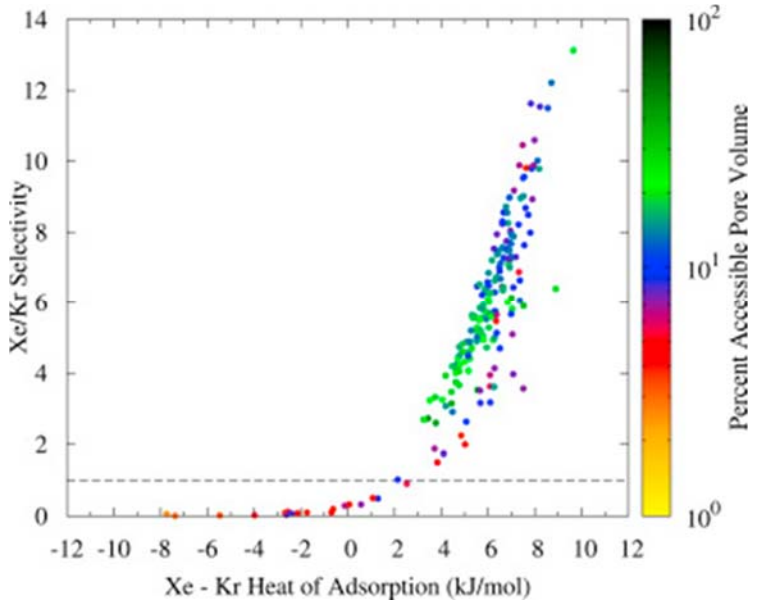

Figure 19: Selectivities as a function of difference in HOA.

Compiling the most selective materials at the both initial and high loadings, we selected 23 frameworks for more detailed study: AFO, {ATN}, ATO, BOF, CAN, {CDO}, EAB, EDI, EON, EPI, ESV, {FER}, {LAU}, LTF, MAZ, {MRE}, MTF, OFF, OWE, {PCR}, {PSI}, UFI, and {ZON} (those in bold are among the most selective at both initial and final loading). Examining these structures, we have identified two different sets of adsorption behavior that correspond with distinct structural motifs responsible for the high selectivity. The first category of selective zeolite frameworks, comprising the majority of the best performers, exhibits flat or slightly increasing selectivity and is associated with a narrow pore system. The remaining highly selective zeolites exhibit a high initial selectivity which drops, often dramatically, as loading increases. This type of behavior is associated with the presence of small pockets capable of adsorbing a single gas atom that are accessible off larger channels.

The first group, where selectivities increase or remain nearly constant as a function of loading, contain narrow pore systems. We later showed that porous transition metal formates exhibit among the highest selectivities Kr/Xe selectivities reported, and that this selectivity gently improves with increased loading, due to this mechanism.[3] This result was further enforced by a recent survey of 670,000 materials by Smit and co-workers, which did analyze the IZA zeolites but only for initial selectivity.[7] ATN is an example of a narrow channel pore system with 1-D, 6Å diameter pores. The Xe loading is centralized in the t-ocn (atn) composite building unit (CBU) maximizing the Xe atoms dispersion interaction with the two 8-ring windows of the t-ocn (Figure 20a). The constricted pores provide a site (or sites) with a large amount of contact between the pore wall and the adsorbed gas, leading to high dispersive interactions good selectivity. Typically, only one or

several crystallographically distinct gas adsorption sites are present in compounds with this type of adsorption. If only one site is present, the only energetic difference between the first gas molecule to adsorb and the last are fluid-fluid interactions, resulting in a gradual increase in HOA and selectivity. While slightly more complicated, similar overall behavior generally occurs when several adsorption sites are present, especially with the sites are chemically similar. 8-ring pores are common in this group with examples of cylindrical, elliptical or zig-zag cross sections. 10-ring pores tend to be distorted. The zeolites EPI, ESV, MTF, and OWE show fall-offs in selectivity at high loadings. OWE and EPI are 2-dimension materials with limited wall surface for adsorption whereas ESV and MTF have undulating pore volumes that resemble a series of pockets connected by smaller windows. As these features saturate, the decrease in selectivity is observed.

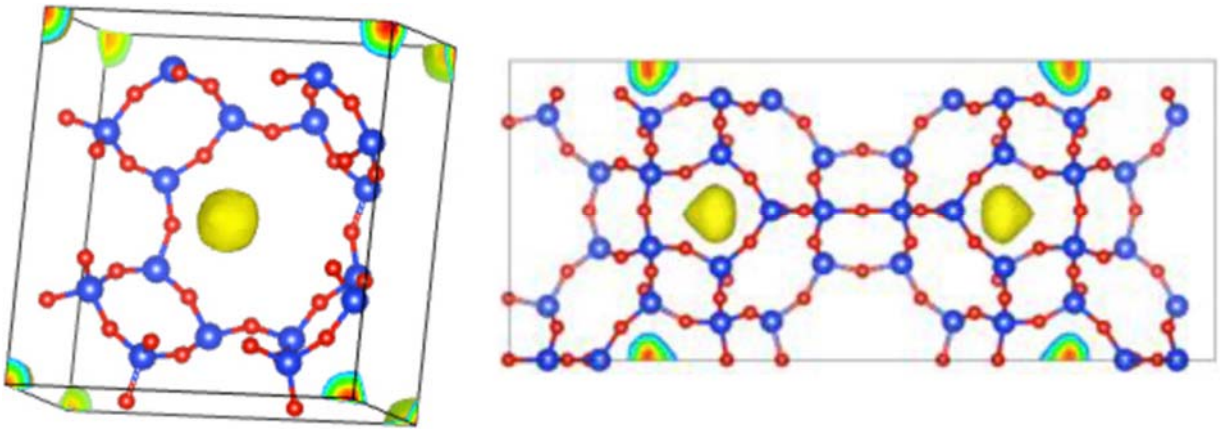

Figure 20: Most probably gas occupancy sites in the zeolites a) ATN and b) UFI.

The second category of topological features leading to high selectivity are small pockets or secondary pores connected to larger pores. Features comparable in size to Xe provide a region with very high dispersive interactions favoring Xe. We have previously shown that this is the mechanism behind high initial HOAs and selectivities for Kr and Xe in HKUST-1, but that it also leads to lower HOAs and selectivities at higher loadings. In our survey, this mechanism leads to the highest initial selectivities, but these may not be ideal adsorbents for PSA-type processes as the selectivities drop as loading increases. We illustrate this mechanism with UFI, which has the highest predicted initial selectivity for siliceous zeolites. UFI has a 2D pore system consisting of large lta cages connected through 8-ring pores. A number of t-ufi cages are accessible through this pore system; this is where the simulations show gas density building up at low loadings (Figure 20b). This is analogous to the mechanism for high initial selectivity observed in HKUST-1.

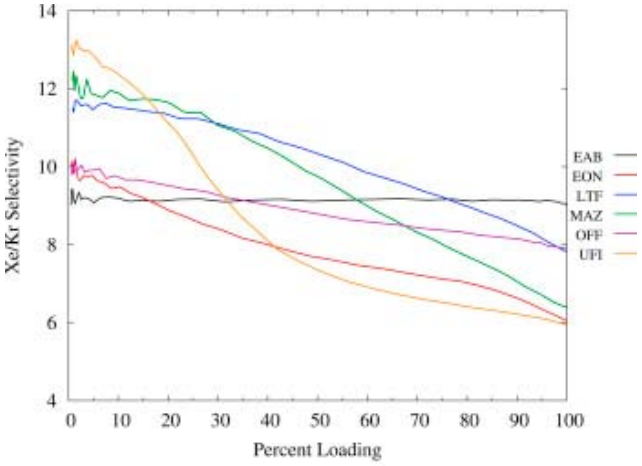

(a) Zeolites with small cages

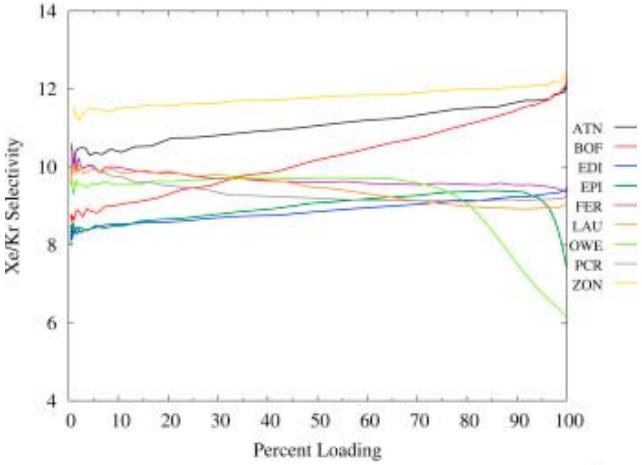

(b) Zeolites with channels and loading $\geq$ 45 cm^3/g

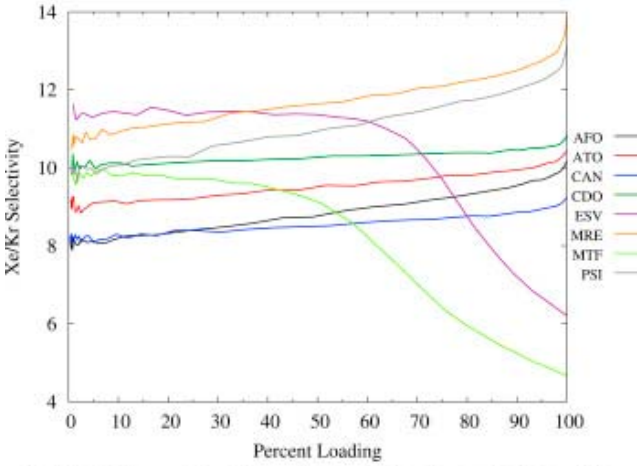

(c) Zeolites with channels and loading $\leq$ 45 cm^3/g

Figure 21 (prev page) shows the results from the more thorough selectivity simulations for each of the top zeolites as a function of percent loading, with 100% defined as the respective loading at 10,000 mmHg. As all of the simulated adsorption data has been corrected to reflect the excess adsorption, a turnover in the isotherm should be expected when the density of the adsorbed fluid very closely matches that of the bulk fluid. By collecting some data points beyond 10,000 mmHg, we have determined that this turnover occurs around 10,000 mmHg in almost all of these zeolites thus indicating the loading at 10,000 mmHg is close to the asymptotic limit. The results have been divided into two sets corresponding to either narrow pores or cavities off larger pores, and for visual clarity the narrow pore materials have been further sub-divided based off of their loading at 10,000 mmHg. Note that the noise at low loadings is due to very low total Kr uptake.

Each of the materials with a small pocket adsorption mechanism are shown in Figure 21a. In these materials, small cages accessible from larger channels result in high initial selectivities as these pockets fill. Once the majority of the pockets have filled, larger fractions of adsorbed gas atoms occupy less selective sites in the larger pores, leading to lower selectivities at higher loadings. For example, the t-ufi cages in UFI are nearly saturate at 10-2% of the total possible loading. Once the t-ufi cages are close to saturated, the majority of the adsorption occurs in the t-grc cages. These t-grc cages are not expected to be as selective based on our screening results for LTA, which only can adsorb into t-grc CBUs and has a selectivity of 4.5 at all loadings. Interestingly enough, UFI had the highest capacity of any of the zeolites closely examined at 88.0 cm^3/g. An exception to dramatically falling selectivities is EAB where the selectivity remains essentially flat across all selectivities studied. As EAB contains large channels that connect smaller t-gme pockets off the main pores, this behavior came as a surprise. Examining predicted adsorption sites, Xe indeed occupies the t-gme pocket as anticipated, but also occupies two well-defined sites in the larger t-eab cavities of the main pore. This is the only instance we are aware of where a pocket large enough to accommodate two Xe atoms provides comparable selectivities to a pocket which only accommodates one.

The GCMC results presented above represent a significant step towards identifying zeolitic adsorbents for practical separations, although more than was determined above will ultimately be required. Practical adsorbents need to be available economically and show reasonable kinetics. While the selectivities as over useful loading ranges are most promising with narrow pore zeolites, these zeolites may also show much lower adsorption/desorption kinetics compared with zeolites containing larger pores and selective pockets. EAB represents a potentially important framework as it has both large channels, which should lead to superior kinetics, and also flat selectivity at all loadings. Further experimental studies are needed to determine whether these zeolites would be practical in real-world separations.

We are also well-aware that most zeolite frameworks have not been synthesized in purely siliceous forms. To our surprise, a number of zeolites do exhibit selectivities that are competitive with the best MOF adsorbents studied so far. One of the promising structures to emerge from this effort is FER, which is well-known in a pure silica form. Other frameworks (e.g. MRE, UFI) occur in high Si/Al ratios, as germanosilicates (e.g. PCR), or as an AlPO (e.g. ATO, ZON), where performance may be comparable to the pure silica form. The promising germanosilicates and pure AlPO results here should be transferable as they have no mobile cations, the dispersion interactions should be similar (especially if the T-atom approximation is made), and the distribution of framework partial charges will have little effect on the adsorption of noble gases as polarizability

only accounted for 1-2% of the total energetics in this study (owing to the cancellation of electric fields caused by neighboring charges). Additionally, H-exchanged versions of these frameworks are likely to offer similar overall performance. Even in cases where compounds resembling the SiO_2 form do not exist, such frameworks remain promising for follow-up studies where mobile cations are present. A final substantial advantage that siliceous zeolites have over aluminosilicates is that they are sufficiently hydrophobic that separations could be run in the presence of humidity without need for periodic reactivation.

The screening results presented here are a first step towards screenings with cations present. For realistic results from such screenings, cation mobility must be included, which represents a considerable challenge on its own. Good agreement between our experimental and simulated data on several SiO_2 structures provides important validation that our model is indeed sufficiently accurate. The screening has also provided important clues as to which frameworks may be promising as cations are included in later simulations. Finally, in order to correlate our results with the recent study by Smit,[7] we compared our predicted performance for air separation (Xe/Kr = 20:80) to results for the radiochemical separation. The Xe selectivities remained comparable, except in compounds showing high selectivity due to small pockets, where the high loading selectivity greatly improved for the 20:80 ratio.

In conclusion, an initial screening demonstrated that many siliceous zeolites have promise for a Kr/Xe separation. In the case of EAB, EON, LTF, MAZ, OFF and UFI, a high initial selectivity results from the presence of a small cage off of the main pore system that is about the right size to adsorb a single Xe atom. However these small cages quickly saturate with increased gas loading. Zeolites with only small cages are expected to have limited utility as practical PSA sorbents as their selectivity is limited by the adsorption into the small cages. The most promising zeolites for selective Xe adsorption at PSA relevant pressures were ones that contained narrow pore systems with either zig-zags or elliptical cross sections. We suggest the most promising topologies for further study are CDO, MRE, and PSI as they have selectivities greater than 10 at all loadings and high capacities. CDO, FER, MRE, and MTF are of particular interest as these frameworks can be made as pure SiO_2. AFO, ATO, PSI, and ZON are also of interest as they can be made as pure AlPOs to test the transferability of the pure silica results.

It is also important to note that a good parametrization of the force field is essential to using multi-component GCMC as a screening tool. TraPPE-zeo provides an excellent transferable description of fluid-framework interactions. The fluid-fluid interactions need to be correctly modeled to get good isothermal agreement at both low and high loadings, in particular for Kr/Xe a softer repulsion term than that of a 12-6 Lennard-Jones is needed. This problem is not unique to this work, and can be seen in many of the previously published Kr/Xe adsorption isotherms into MOFs and zeolites. In the future, we intend to extend our findings to some of the more complex zeolitic topolgies, i.e. cation containing aluminosilicates, and to include framework flexibility to better describe materials known to distort on adsorption like MFI.

4.5 Grand Canonical Monte Carlo Simulations

Much of our work in developing GCMC simulations to guide our experimental efforts is included in sections. As part of our investigation into Kr/Xe separations, we have developed an approach that combines straightforward single gas adsorption isotherms with multi-gas high throughput computation that provides accurate selectivities across a wide range of conditions. Application of this methodology to seven different metal-organic frameworks demonstrates that it is possible to calculate selectivity over wide ranges of conditions and provides a far more useful assessment than a simple initial selectivity.

Given the accuracy with which GCMC has been shown to match experimental single gas data, it is reasonable to anticipate that GCMC will calculate binary gas adsorption, and thus quantities such as selectivity, with comparable accuracy. We used an automated scripting environment to carry out large numbers of simulations, enabling selectivity to be evaluated over a range of conditions. For each MOF investigated, 4797 selectivities were simulated from 200-320K at 10K intervals with a range of pressures between 0.01 torr to 5 atm. The Xe/Kr mole fractions were analyzed at 10\% intervals. Selectivity turns out to depend appreciably on the composition of gas. The 50/50 gas mixture typically had the median selectivity. The selectivity for the other mole fractions deviated by more than of 20% of the value for the 50/50 gas mixture in some cases. Clearly, selectivity needs to be measured for gas mixtures of comparable composition of those that will be used in the separation. Given the large amount of data collected, we will confine our analysis to the gas mixture of interest (90/10 Xe/Kr). Partial results are presented in Figure 22 and 23. We are presently revising this work for resubmission soon.

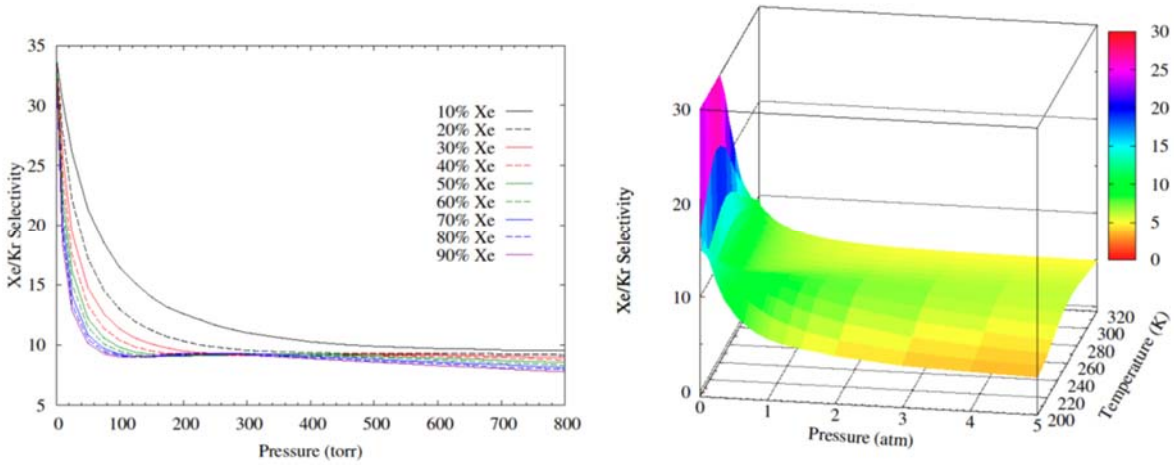

Fig 22: Composition-dependent selectivity curves for HKUST-1 (left), showing how dramatically the selectivity changes as a function of composition and loading. The plot on the right shows a 3D surface with selectivity varying as a function of temperature and pressure for a fixed gas composition (50%/50%)

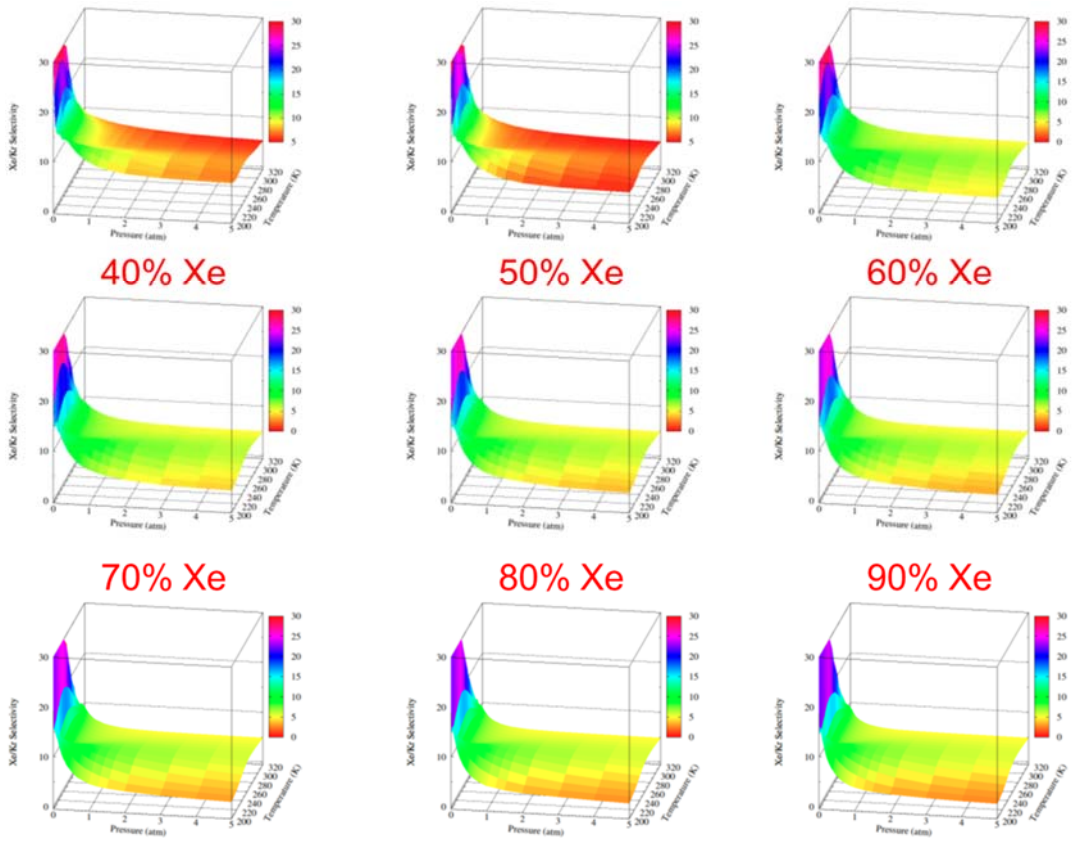

Figure 23: 3D selectivity surfaces for 9 different gas compositions, representing nearly 4800 specific selectivity calculations.

Multi-component GCMC simulations provides an excellent tool for screening materials for generating situation-specific selectivities needed to develop processes. Care needs to be given to the Hamiltonian used in the simulations and its parametrization (*i.e.* force field selection) to ensure that any discrepancies between theory and experiment are minimized, and comparable for each gas in the mixture. We have identified a good force field / polarizability parametrization for the separation of Kr/Xe in seven different MOF materials; we anticipate that this parametrization should be robust for simulating Kr/Xe separation in other MOF families. Using an accurate description of the structure is also critical, particularly when features critical to adsorption are comparable in size to the adsorbed phase. Our observations of appreciably different behavior depending on which crystallographic structural model were used in HKUST-1 suggest that choice of proper model may be critical. A solution to this issue may be development of Monte Carlo codes capable of including optimization of the structure of the adsorbent in response to gas adsorption.

Kr/Xe selectivity varies greatly depending on thermal conditions and the material being analyzed, and initial selectivities are not sufficient to predict a material's performance in a PSA

application. By evaluating how selectivities vary according to the variables that we studied, we have demonstrated the importance of obtaining experimental selectivities at conditions as close as practical to the conditions that will be used in the separation.

4.6 Publications/Presentations

The following publications have appeared (so far). We are still working on several additional papers from existing results.

1. "Assessing Zeolite Frameworks for Noble Gas Separations Through a Joint Experimental and Computational Approach" Keith V. Lawler, Amit Sharma, Breetha Alagappan, Paul M. Forster*, *Microporous Mesoporous Mater.* **2016,** 222, 104-112 doi:10.1016/j.micromeso.2015.10.005

2. "On the Importance of a Precise Cyrstal Structure for Simulating Gas Adsorption in Nanoporous Materials" Keith V. Lawler, Zeric Hulvey, Paul M. Forster*, *Phys. Chem. Chem. Phys.,* **2015**, 17, 18904-18907 **DOI:** 10.1039/C5CP01544H

3. "Nanoporous Metal Formates for Krypton/Xenon Separation" Keith V. Lawler, Zeric Hulvey, Paul M. Forster*, *Chem. Comm*., **2013,** 49, 10959-10961. DOI: 10.1039/c3cc44374d

4. "Noble Gas Adsorption in Copper Trimesate, HKUST-1: An Experimental and Computational Study" Zeric Hulvey, Keith V. Lawler, Zhiwei Qiao, Jian Zhou, David Fairen-Jimenez, Randall Q. Snurr, Sergey V. Ushakov, Alexandra Navrotsky, Craig M. Brown, Paul M. Forster* *J. Phys. Chem. C.,* **2013**, 117, 20116-20126. 10.1021/jp408034u

In addition, this work has been the major portion of the following oral presentations:

1. [Invited] "A Computationally-Driven Approach to Identifying Materials for Gas Separations" UNLV Department of Chemistry and Biochemistry, Las Vegas, NV, September 19, 2014.

2. "Establishing an Atomistic Picture of Gas Sorption With and Without Crystallography: Tools for Advanced Separations" Paul M. Forster, American Crystallographic Association National Meeting, Albuquerque, NM, May 26, 2014.

3. [Invited] "Establishing an Atomistic Picture of Gas Sorption Without Crystallography: Tools for Advanced Separations" Paul M. Forster, Argonne National Laboratory, Argonne, IL, March 20, 2014.

4. [Invited] “Establishing an Atomistic Picture of Gas Sorption Without Crystallography: Tools for Advanced Separations” Paul M. Forster, Cleveland State University, Cleveland, OH, February 20, 2014.

5. [Invited] “Establishing an Atomistic Picture of Gas Sorption Without Crystallography: Tools for Advanced Separations” Paul M. Forster, Oberlin College, Oberlin, OH, February 19, 2014.

6. [Invited] “Establishing an Atomistic Picture of Gas Sorption Without Crystallography: Tools for Advanced Separations” Paul M. Forster, Stony Brook University, Stony Brook, NY, February 17, 2014.

7. “Sorbents for Kr/Xe Separations” GLOBAL 2013: International Nuclear Fuel Cycle Conference, Salt Lake City, UT, Sept. 29 – Oct 3, 2013.

8. [Invited] “Kr/Xe Separations in Nanoporous Hosts: A Combined Experimental and Computational Approach” Paul M. Forster, ACS National Meeting, Indianapolis, IN, Sept. 10, 2013.

9. [Invited] “Establishing an Atomistic Picture of Gas Sorption Through Complimentary Experimental Techniques” Paul M. Forster, The George Washington University, Washington DC, Oct 24, 2013.

10. [Invited] “Establishing an Atomistic Picture of Gas Sorption Through Complimentary Experimental Techniques” Paul M. Forster, Georgetown University, Washington DC, Oct 25, 2013.

11. [Invited] “Kr/Xe Separations in Nanoporous Hosts: A Combined Experimental and Computational Approach” Paul M. Forster, ACS National Meeting, Indianapolis, IN, Sept. 10, 2013.

12. [Invited] “Towards Improved Frameworks for Gas Separations: Establishing an Atomistic Picture of Gas Sorption Through Complimentary Experimental Techniques” Paul M. Forster, American Crystallographic Association Meeting, Honolulu, HI, July 23, 2013.

13. [Invited] “Solid State Chemistry Relevant to the Nuclear Fuel Cycle” Paul M. Forster, Rutgers University, Rutgers, NJ, Aug. 23, 2012.

14. [Invited] “Characterization of Nanoporous Sorpents for Noble Gas Separations,” Paul M. Forster, Zeric Hulvey, Keith Lawler, ACS National Meeting, Philadelphia, PA, Aug. 22, 2012.

15. [Invited] “Technetium Chemistry at UNLV” Paul M. Forster, Frederic Poineau, Erik V. Johnstone, Efrain E. Rodriguez, Alfred P. Sattelberger, Philippe Weck, Kenneth R. Czerwinski, Department of Chemistry, Loughborough University, UK, July 11, 2011.

16. [Invited] “Applications of Nanoporous Materials in Gas Separations and Storage” Paul M. Forster, Micromeritics Instrument Corporation, Norcross, GA, January 17, 2011.

---

1. “Noble Gas Adsorption in Copper Trimesate, HKUST-1: An Experimental and Computational Study” Zeric Hulvey, Keith V. Lawler, Zhiwei Qiao, Jian Zhou, David Fairen-Jimenez, Randall Q. Snurr, Sergey V. Ushakov, Alexandra Navrotsky, Craig M. Brown, Paul M. Forster* *J. Phys. Chem. C.,* **2013**, 117, 20116-20126. 10.1021/jp408034u

2. “On the Importance of a Precise Cyrstal Structure for Simulating Gas Adsorption in Nanoporous Materials” Keith V. Lawler, Zeric Hulvey, Paul M. Forster*, *Phys. Chem. Chem. Phys.,* **2015**, 17, 18904-18907 **DOI:** 10.1039/C5CP01544H

3. “Nanoporous Metal Formates for Krypton/Xenon Separation” Keith V. Lawler, Zeric Hulvey, Paul M. Forster*, *Chem. Comm*., **2013,** 49, 10959-10961. DOI: 10.1039/c3cc44374d

4. “Assessing Different Zeolitic Adsorbents for their Potential Use in Kr and Xe Separation” Breetha Alagappan, University of Nevada Las Vegas.
http://digitalscholarship.unlv.edu/cgi/viewcontent.cgi?article=2968&context=thesesdissertations

5. “Assessing Zeolite Frameworks for Noble Gas Separations Through a Joint Experimental and Computational Approach” Keith V. Lawler, Amit Sharma, Breetha Alagappan, Paul M. Forster*, *Microporous Mesoporous Mater.* **2016,** 222, 104-112 doi:10.1016/j.micromeso.2015.10.005

6 C. A. Fernandez, J. Liu, P. K., Thallapally, D. M., Strachan, *J. Am. Chem. Soc.,* **2012**, 134, 9046-9049.
7 C.M. Simon, R. Mercado, S.K. Schnell, B. Smit, M. Haranczyk, *Chem. Mater*. **2015**, p. 4459-4475
DOI: 10.1021/acs.chemmater.5b01475